Pergamon

Cement and Concrete Research, Vol. 25, No. 4, pp. 741-751, 1995

0008-8846/95 $9.50+.00

0008-8846(95)00064-X

MODELLING OF THE TRANSITION ZONE POROSITY

B. Bourdette*, E. Ringot** and J.P. Ollivier**

*Department of Waste Storage and Disposal
Atomic Energy Commission, Gif-sur-Yvette France

**LMDC, INSA-UPS, Toulouse France

(Refereed)
(Received April 4, 1994; in final form March 7, 1995)

ABSTRACT

The ion diffusion process in mortar is different from the one which occurs in cement paste. This difference is due to the presence of transition zones, which take place around the grains in mortar and which are very porous regions. Based on mercury intrusion porosimetry experimental data and on the analysis of percolation through a 3D mortar model, a computation of the transition zone porosity and of the bulk paste porosity has been carried out. The porosity of the transition zone has been analyzed as a function of the mortar composition and of the degree of hydration.

INTRODUCTION

Concretes and mortars are heterogeneous materials composed of aggregates, cement paste and water. The microstructure of cement paste in the vicinity of an aggregate particle in mortar or concrete differs from the bulk cement paste. This interfacial region, called "auréole de transition" or transition zone, is an integral part of the whole microstructure so it is difficult to characterize each feature of this zone.

It is well known that the porosity is the phase with the greatest importance for the durability of cementitious materials. Aggressive substances are transported into the materials in the liquid state through the complex porous system. The transition zones are very porous (1,2,3) and if they are connected by overlap or by microcrack formation, they create a network where aggresive ions can diffuse easily (4,5). To understand the degradation of mortars or concretes by aggressive solutions or by slightly ionized water, it is necessary to know the role played by transition zones in the ion diffusion phenomenon into the cementitious composites. Thus, one has to determine the transition zone porosity.

Some scientists (1,2,3,6) have shown using different techniques that the transition zone porosity is higher than the bulk cement paste porosity, but they could not determine exactly the interfacial zone porosity volume. Bentz, Garboczi and Stutzman (8) have carried out a digital-image-based model, to simulate cement paste-aggregate interfacial zone microstructural development. By this

model they could compute the porosity fraction of the cement paste as a function of distance from the aggregate surface.

We have developed another model which allows, coupled with mercury intrusion porosimetry data, the evaluation of the total transition zone porosity, as a function of the cementitious composite composition and the degree of hydration. This study is focused only on mortars.

MATERIALS AND EXPERIMENTAL METHOD

Materials

The cement used in preparing mixes for these investigations was an ordinary portland cement (OPC). The chemical composition of the cement is presented in table 1.

Table 1
Chemical Composition of Cement

Oxide	CaO	SiO_2	Al_2O_3	Fe_2O_3	SO_3
Content(%)	62.9	20.6	5.8	3.6	3.1

An inert, clean quartz sand of two different size gradations was used : 0.16/2 ; 0.16/3.15 mm.

Preparation of mortar materials

Incidentally, two mortars have been used for this study. They have the following characteristics (table 2).

Table 2
Characteristics of Mortar Materials

Mortar	M1	M2
W/C	0.4	0.5
Particle size (mm)	0.16/3.15	0.16/2.0
Sand volume fraction (%)	52	57

The mortars have been cast into cylinders (110 mm diameter and 220 mm height), and then demolded and cured at 20°C in lime-water for different periods of time.

Mercury intrusion porosimetry (MIP)

The model presented in this paper has been developed to link transport properties of cementitious composites with their porosity and to take into account the features of the interfacial zone. Consequently, the pore diameter distribution used in this model is that obtained by mercury intrusion porosimetry, because this technique is also a transport analysis of the porous structure.

A standard porosimeter (Micromeritics Autopore II 9220) which allows the application of pressures up to 415 MPa has been used. This corresponds to a minimum radius of 3 nm. The radius r of pores, which can be penetrated by mercury at pressure P, can be related by equation (1).

$$r = -\frac{2\,\sigma\cos\theta}{P} \qquad (1)$$

where σ is the surface tension of mercury and θ the solid-mercury contact angle (130°). The pore-size measurements have been carried out on small pieces (about 2 cm^3) of mortar pre-dried under vacuum at room temperature.

MODELLING OF THE INTERFACIAL ZONE POROSITY

Hypotheses

⇨ the sand grains are spherical.

⇨ because the interfacial zone has a nonuniform geometry, it is difficult to determine exactly its thickness. We have found in the literature (1,2,6,7) that the principal variations of porosity and concentration occur with a distance of 30 μm from the aggregate surface. Thus, we estimate that whatever :

- the aggregate size (8),
- the W/C ratio (9),
- the sand volume fraction (10),
- the age of mortar (the degree of hydration),

⇨ the interfacial zone thickness is constant and equal to 30 μm for an ordinary portland cement (OPC).

⇨ the composite mortar structure is divided into three parts (figure 1) :

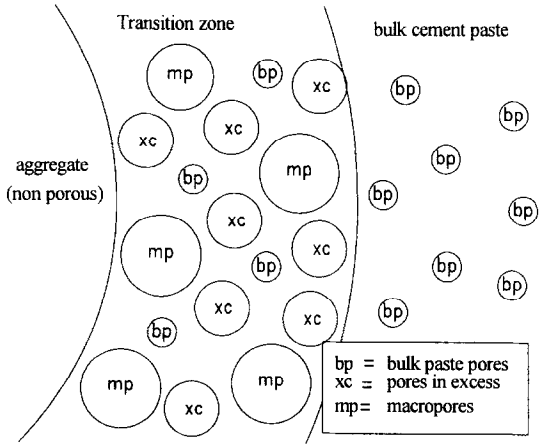

FIG. 1
Finite schematic volume representation of composite mortar structure

- aggregates
- the bulk cement paste

- transition zones which are constituted by a cement matrix and macropores (pores with diameters contained between 0.1 and 5 μm). According to the Monteiro's model (11) of the transition zone, one can assume that the cement matrix in the interfacial zone has the same void distribution as the bulk cement paste with a porous volume in excess for the pores bounded by 0.045 and 0.1 micrometers when we neglect the crystals in direct contact with the aggregate (figure 2).

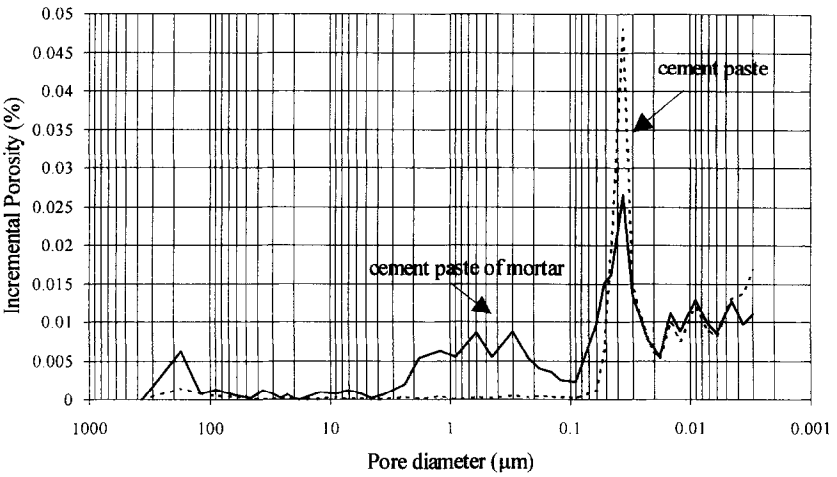

FIG. 2
Incremental porosity distribution of pure cement paste W/C 0.4
and cement paste of mortar M1 (3 months old)

Model

The transition zone porosity ϕ_{tz} is defined by

$$\phi_{tz} = \frac{V_{Vtz}}{V_{tz}} \tag{2}$$

where V_{tz} is the transition zone volume and V_{Vtz} the void volume contained in V_{tz}.

To calculate ϕ_{tz}, we have to determine V_{tz} and V_{Vtz}.

Determination of Vtz contained in mortar volume V_M :

According to the sand granulometric curves (figure 3), we deduce the number of sand grains N_{ig}, contained in each class in the case where all grains in a class have the same average diameter d_i, for a mortar volume V_M.
Knowing that around each grain there is an interfacial zone of 30 μm thickness, we determine the transition zone volume V_{itz} for each class. Apart from the overlapping volume between all the interfacial zones, the total transition zone volume V'tz contained in V_M is equal to :

$$V'_{tz} = \sum_{i=1}^{n} V_{itz} \qquad \text{with i=1..n the number classes} \tag{3}$$

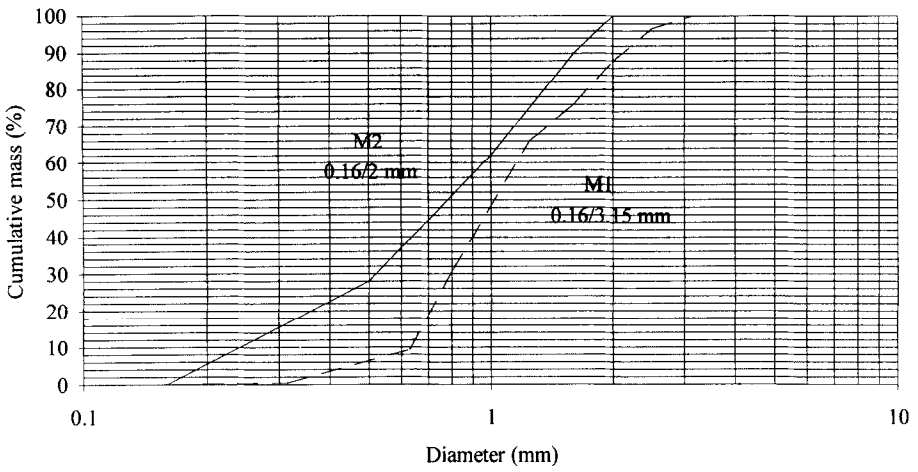

FIG. 3
Particle size distribution of quartz sand 0.16/2 and 0.16/3.15 mm

We have to take account that some transition zones are connected and then they overlap each other.

We define the transition zone volume Vtz to be equal to the interconnected interfacial zones volume Vtzc plus the non interconnected transition zones volume Vtznc :

$$V_{tz} = V_{tzc} + V_{tznc} \tag{4}$$

The interconnected transition zones fraction is defined by the ratio :

$$\frac{V'_{tzc}}{V'_{tz}} = x \tag{5}$$

where V'tzc is the total interconnected transition zones volume in which the overlapping volume is not deduced. The common interfacial zones volume is denoted by Vc, thus its fraction is :

$$\frac{V_c}{V'_{tzc}} = y \tag{6}$$

When the transition zones are connected we have to substract the common transition zone volume Vc from the total interconnected interfacial zones volume, then the interconnected transition zones volume is equal to :

$$V_{tzc} = V'_{tzc} - V_c = x\,(1 - y)\,V'_{tz} \tag{7}$$

The non interconnected interfacial zones volume is defined by :

$$V_{tznc} = (1 - x)\,V'_{tz} \tag{8}$$

Then, we deduce that the transition zone volume used in the model is equal to :

$$Vtz = (1 - x.y)\ V'tz \quad (9)$$

Now, we have to determine x and y.

Generation of the 3D mortar model

The model used for the generation of mortars is quite similar to Snyder's (10). In this model, each class of aggregates is replaced by one set of identical hard spheres in respect to the real volume it occupies. The spheres are placed in the volume, the biggest ones first, then the smaller. The centers are chosen randomly and no sphere can overlap another one. If a corner, an edge or a side of the parallelepipedic volume of the digital sample is intercepted, periodic conditions are applied in order to limit boundary effects.

The interfacial zone is modelled by a surrounding spherical volume centered on each grain with a unique typical 30 μm thickness.

A program "genb3d" has been written (C language on Unix system) which generates a 3D mortar model based on the dimensions of the sample, the composition, and the granular gradation. It has been used to produce both M1 and M2 mortars in several 10x10x10 mm^3 cubes.

Analysis of the interfacial zone connectivity

Each grain is implemented as a data structure which contains, among other characteristics, the grain radius, its centroid position and the transition zone thickness. A program "iztb3d" allows us to change this thickness, enabling a study of the influence of this parameter on the results.

The algorithm used to find a percolation path through the interfacial zones differs from the burning algorithm introduced by Stauffer (14). We have instead written a recursive procedure in which clusters of overlapping transition zones are identified. During computation, tests are

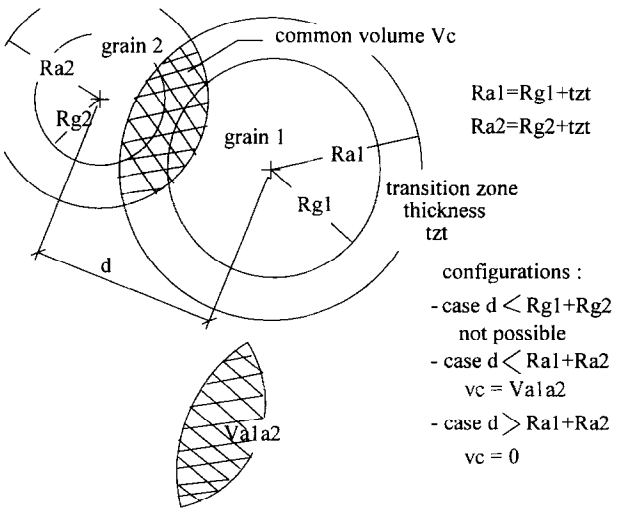

FIG. 4
Common transition zone volume of two neighbouring grains

performed to check if the current cluster extends from a side of the sample to the opposite side. Each cluster is numbered and the percolation clusters, if they exist, are especially marked.

The volume of each cluster is evaluated as the sum of all the connected transition zones volumes in the cluster.

In order to evaluate the maximum error made on the volume of clusters, the analysis program "anab3d" also computes the overlapping volume v_c of all pairs of neighboring grains (figure 4).

The sum extended to all the pairs of neighbors in the clusters is $V_c = \Sigma v_c$

But, V_c is always above the real error because more than two transition zones may share a common volume. Hence, we have : real $V_{tz} \rangle V_{tz} - V_c$

The results (table 3), obtained from 10 calculations, show that the error is always less than 5.5% for M1 and 20% for M2.

Table 3
Results of the connectivity analysis

Mortar	M1	M2
V'_{tz} (mm^3)	95.45	201.14
x (%)	96.98	99.92
y (%)	5.5	20

2D Visualization

Among others features developed with the model, we have written two programs, "secb3d" which allows one to define a section in the sample and "dispb3d" which displays the cross section on an XWindow terminal.

An example of this output is given in figure 5 for the mortar M1. The grains which belong to the percolating cluster are drawn in light grey and the other ones in dark grey. The traces of the transition zones, in black, have different thicknesses because they result from the intersection of a spherical shell with the cutting plane.

In spite of the high connectivity of both the mortars M1 and M2, two-dimensionnal images do not reveal any obvious continuous pathway from a side to the opposite one, through the interfacial zones. This fact confirms the difficulty in studying the structure of materials from cross sections which often give an erroneous view of the three-dimensional reality.

Determination of ϕ_{tz} :

We have defined two porosities, ϕ_{mp} and ϕ_{xc} which are respectively the porosities generated by the macropores (0.1 - 5 μm) and the pores in excess (0.045 - 0.1 μm) :

$$\phi_{mp} = \frac{V_{Vmp}}{V_{tz}} \qquad (10) \qquad\qquad \phi_{xc} = \frac{V_{Vxc}}{V_{mtz}} \qquad (11)$$

where V_{Vmp} and V_{Vxc} are respectively the volumes of the macropores and of the pores in excess,

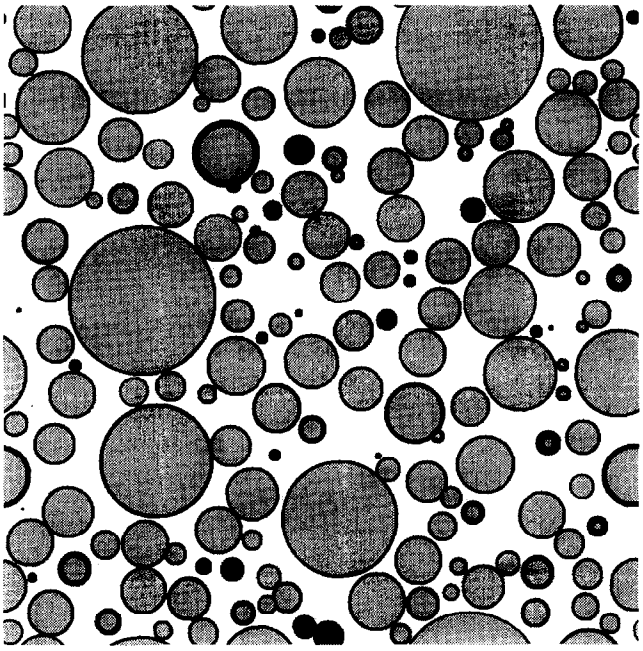

white : bulk paste **black** : transition zone
light grey : grains in the percolating path **dark grey** : others grains

FIG. 5
2 D-visualisation of mortar M1 (10x10 mm² cross section)

and V_{mtz} is the volume of cement matrix of the transition zone. V_{vmp} and V_{vxc} are defined as all transition zones can be accessible by mercury.

As the transition zone contains only the macropores and a cement matrix, the interfacial zone porosity is given by the equation 12.

$$\phi_{tz} = \phi_{mp} + [(1 - \phi_{mp})\, \phi_{mtz}] \tag{12}$$

where ϕ_{mtz} is the porosity of cement matrix of transition zone.

Moreover, the cement matrix of the transition zone is more porous than the bulk cement paste because it contains the pores in excess. We deduce the following equation :

$$\phi_{tz} = \phi_{mp} + [(1 - \phi_{mp})\, \phi_{xc}] + [(1 - \phi_{mp})\, (1 - \phi_{xc})\, \phi_{bp}] \tag{13}$$

where ϕ_{bp} is the bulk cement paste porosity.

We have supposed that sand grains are not porous, and thus the voids in a mortar are contained in the bulk cement paste and the transition zones :

$$\phi_M\, V_M = \phi_{bp}\, V_{bp} + \phi_{tz}\, V_{tz} \tag{14}$$

where ϕ_M is the mortar porosity, and V_M and V_{bp} the volumes of the mortar and of the bulk cement paste.

To determine ϕ_{bp}, ϕ_{tz} in equation (13) is replaced by its expression (equation (14)) :

$$\phi_{bp} = \frac{\phi_M V_M - [\phi_{mp} + (1 - \phi_{mp})\phi_{xc}] V_{tz}}{(1 - \phi_{mp})(1 - \phi_{xc}) V_{tz} + V_{bp}} \quad (15)$$

Finaly, the transition zone porosity is equal to :

$$\phi_{tz} = \phi_{mp} + (1-\phi_{mp})\phi_{xc} + \left((1-\phi_{mp})(1-\phi_{xc}) \left(\frac{\phi_M V_M - [\phi_{mp} + (1-\phi_{mp})\phi_{xc}] V_{tz}}{(1-\phi_{mp})(1-\phi_{xc}) V_{tz} + V_{bp}} \right) \right) \quad (16)$$

Model applications and discussion

Determination of the ratio $Q = \phi_{tz}/\phi_{bp}$:

Results of the interfacial zone porosity model for the mortar M1 (curing 3 months in lime-water) appear in table 4 :

Table 4

Mortar	M1
ϕ_{bp} (%)	19 ± 1
ϕ_{tz} (%)	48 ± 2
$Q = \phi_{tz}/\phi_{bp}$	2.5 ±0.3

We note that the transition zone has a very high porosity, it is about 3 times more porous than the bulk cement paste. These results agree with the experimental results of Scrivener et al. (1) which have shown that the ratio Q is approximatively equal to 3 for a mortar similar to M1.
These results confirm that :

- the wall effect generates the formation of very porous zones around aggregates (3,12)
- the water/cement ratio is higher in the interfacial zone than in the rest of the paste, because there is water accumulation around sand grains resulting from the wall effect and the micro-bleeding water (13).

Moreover, we can see that the bulk cement paste porosity (19%) is lower than the porosity of cement paste (22%) with the same ratio W/C. It is the result of the water accumulation around aggregates which creates water impovershiment in the bulk cement paste and thus decreases its porosity.

Evolution of the ratio Q with the degree of hydration :

This study has been performed with samples of mortar M2. Each mortar was demolded and cured in lime-water for either 1, 3, 6 on 12 months.

Figure 6 shows the evolution of interfacial zone porosity and of bulk cement paste porosity with the age of mortar.

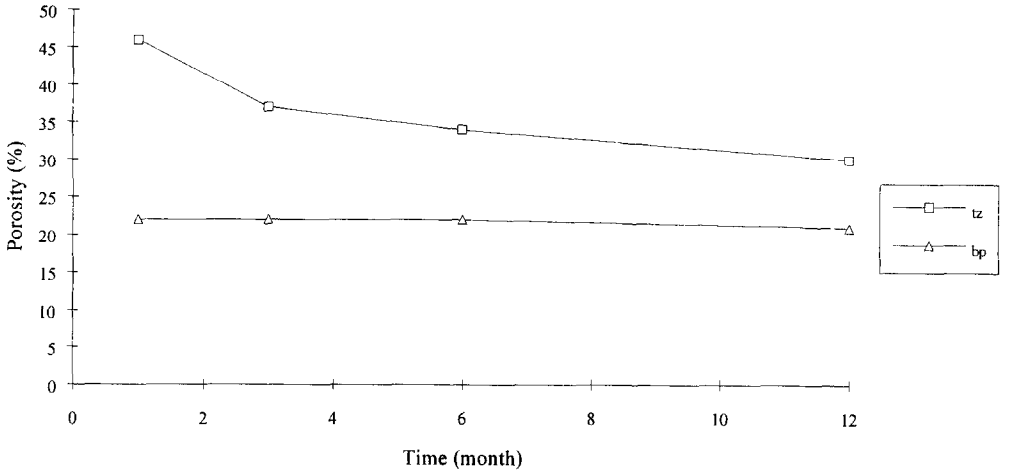

FIG. 6
Evolution of interfacial zone porosity (tz) and of bulk cement paste porosity (bp) with the age of mortar

We notice that the transition zone porosity decreases during the maturation of the material whereas the bulk cement paste porosity remains relatively constant. These trends can be explained by different phenomena. Ion diffusion, due to porosity gradients, from the bulk cement paste to the transition zones (4,6) where precipitation occurs, and the water excess around aggregates (4) which permits anhydrous cement grains to finish their hydration, contributes to decrease the interfacial zone porosity. As the bulk cement paste contains less water than the transition zone, hydration kinetics are lower and its porosity does not vary much with the age of mortar. These phenomena imply that the Q ratio decreases with the degree of hydration as shown in table 5.

Table 5
Evolution of the Q ratio with the age of mortar

Time (month)	ϕ_{bp}	ϕ_{tz}	Q
1	22 ± 1	46 ± 1	**2.1 ± 0.1**
3	22 ± 1	37 ± 1	**1.7 ± 0.1**
6	22 ± 1	34 ± 1	**1.5 ± 0.1**
12	21 ± 1	30 ± 1	**1.4 ± 0.1**

One can see that Q changes between 1 and 6 months, after which it remains constant and is about equal to 1.5.

CONCLUSIONS

The model presented in this paper allows quantification of the porosity of the transition zone. We have seen that the transition zone porosity is not constant. It depends on the mortar composition and the degree of hydration. A new study will be conducted to monitor the evolution of the transition zone porosity and of the bulk cement paste porosity with the water/cement ratio, the

sand grains content and their particle size distribution. As the transition zone has a very high porosity, one can assume that it plays an important role in the ion diffusion process through mortars, particularly when the interfacial zones are connected.

ACKNOWLEDGEMENT

This work is performed within a contract of collaboration CEA-ANDRA (National Agency for Radioactive Waste Management). The helpful comments of Dale Bentz are appreciated.

REFERENCES

1. K.L. Scrivener, A.K. Crumble and P.L. Pratt, Bonding in Cementitious Materials, MRS, 114, p. 87, S. Mindess and S. P. Shah, USA (1988)

2. K.L. Scrivener and E. Gartner, Bonding in Cementitious Materials, MRS, 114, p. 77,S. Mindess and S. P. Shah, USA (1988)

3. G.C. Escadeillas and J.C. Maso, Ceramic Transactions, Advances in Cementitious Materials, 16, p. 169, S. Mindess, (1990)

4. J.C. Maso, 7ème Congrès Int. de la Chimie des Ciments, p. VII-1/3, Septima, Paris (1980)

5. Y.F. Houst, F.H. Sadouki and F.H. Wittmann, Interfaces in Cementitious Composites, RILEM Proceedings 18, p. 279, J.C. Maso, Toulouse (1992)

6. K.L Scrivener and P.L. Pratt, State of Art Report, RILEM TC 108, in Press

7. J.P. Ollivier, Contribution à l'étude de l'hydratation de la pâte de ciment portland au voisinage des granulats, PhD, Toulouse (1981)

8. D.P. Bentz, E.J. Garboczi and P.E. Stutzman, Interfaces in Cementitious Composites, RILEM Proceedings 18, p. 107, J.C. Maso, Toulouse (1992)

9. R. Zimbelmann, Cement and Concrete Research, 15, 801 (1985)

10. K.A. Snyder, D.N. Winslow, D.P. Bentz and E.J. Garboczi, Interfaces in Cementitious Composites, RILEM Proceedings 18, p. 259, J.C. Maso, Toulouse (1992)

11. P.J.M Monteiro, 8th Int. Congress on the Chemitry of Cement, III, p. 433, Brasil (1986)

12. J. Baron, Le Béton Hydraulique, J. Baron and R. Sauterey, p. 95, Paris (1982)

13. M. Hoshino, Materials and Structures, 21, 336 (1988)

14. D. Stauffer, Introduction to percolation theory, p. 4, Taylor & Francis, London and Philadelphia (1985)